INVITED
TALKS

Moving NMR

Bernhard Blümich and the Aachen team

Institute of Technical and Macromolecular Chemistry, RWTH Aachen University, Germany

A unique aspect of Nuclear Magnetic Resonance is that it is in uninterrupted evolution towards new methodologies, instrumentation and applications since its first experimental verification in condensed matter in 1945. The evolution of conventional NMR seems to follow a path to stronger and homogeneous magnetic fields to make use of higher sensitivity and wider spectral dispersion. At the same time, electronic components become smaller and smaller and software becomes more powerful, leaving the magnet and possibly the rf power amplifier as the volume determining quantities of NMR instruments. Mobile NMR is moving that frontier by introducing small NMR sensors and with it methods capable of dealing with the challenges associated with small magnets.[1] Prominent challenges are low field strength, low field homogeneity, temperature drift of permanent magnets, and low electric power consumption for battery operated measurements.

The evolution of NMR is reviewed and the prominent challenges of mobile NMR are addressed. General solution strategies are outlined and particular solution concepts of the Aachen team are reported together with an overview of novel applications of mobile NMR.

References:

1. B. Blümich, F. Casanova, J. Perlo, *Mobile Single-Sided NMR*, Prog. Nucl. Magn. Reson. (2008) in press, doi:10.1016/j.pnmrs.2007.10.002.

Probing Multi-Component Transport in Porous Media over a Hierarchy of Length-Scales

L. F. Gladden [a], T.C. Chandrasekera [a], Y.Y. Chen [a], J.H.P. Collins [a], C.P. Dunckley [a], E.J. Fordham [b], M.L. Johns [a], M.D. Mantle [a], J. Mitchell [a], M.H. Sankey [a], and A.J. Sederman [a]

[a] University of Cambridge, Department of Chemical Engineering, Pembroke Street, Cambridge CB2 3RA, U.K.
[b] Schlumberger Cambridge Research, High Cross, Madingley Road, Cambridge CB3 0HG, U.K.

Understanding transport processes in porous media is central to the design and operation of many chemical and physical processes. Ongoing work in the group aims to develop a suite of techniques which can probe transport processes in porous media over a hierarchy of length-scales from 10^{-8}-10^{-2} m. This talk will summarise the motivation for applying magnetic resonance techniques to study transport phenomena in a number of different systems, and then present illustrative results. Three areas of application will be considered:

Oil recovery – identifying oil and water fractions in a permeable rock
Recently we have implemented a pulse sequence in which T_1 relaxation times have been encoded in the second dimension of two-dimensional relaxation correlation and exchange experiments using a rapid "double-shot" T_1 pulse sequence. The technique retains chemical shift information (δ) for short T_2^* systems. Thus, a spectral dimension is incorporated into a T_2-T_1-δ correlation without an increase in experimental time compared to the conventional, chemically insensitive T_1-T_2 correlation. This approach enables the unambiguous identification of oil and water fractions in a permeable rock.

Pharmaceutical delivery systems – quantifying rapidly evolving pore-size distributions
For reasons of both ease-of-use for the consumer and more effective treatment, there is increasing motivation to understand and control the release of drug into the body from a 'delivery system'; e.g. tablet, polymer extrudate. Magnetic resonance is well-established for use in characterising pore-size distributions in, for example, rocks – in such systems the pore size is usually constant with time. When considering pharmaceutical delivery systems, the pore size will evolve with time. Recent data will be presented which demonstrate that during release, both the pore structure and the dissolution of the pharmaceutical active can be followed using combined [1]H T_2 relaxometry/ $\boldsymbol{q}$-space molecular displacement imaging and ^{19}F NMR, respectively.

Chemical reaction engineering – velocity mapping of gas and liquid in two-phase flows
The fixed-bed reactor is widely used throughout the chemical industry. The process unit comprises a cylindrical column packed with porous catalyst particles. In the context of this meeting, the fixed-bed reactor can therefore be considered as a model hierarchical porous structure comprising the macroscopic pore space of the inter-particle space within the cylinder, and the micropore space within the catalyst pellets. Here we will focus on recent results in which we have imaged both gas and liquid velocities within the inter-particle space. These data allow us to compare the characteristics of two-phase (gas-liquid) flow with that of a single-phase flow within the same porous structure. Further, these data provide us with first measurements of gas, liquid flow velocity and particle wetting upon which predictive models of reactor performance can be developed.

Observation of Fragile-to-Strong Dynamic Crossover in Confined and Hydration Water and Its Relation to the Liquid-Liquid Critical Point in Supercooled Water

Sow-Hsin Chen
Department of Nuclear Science and Engineering, MIT, Cambridge, MA

We have observed a fragile-to-strong dynamic crossover phenomenon of alpha relaxation time [1,4] and self diffusion constant [4,5] in 1-d and 2-d confined deeply supercooled water. The alpha relaxation time is measured by Quasi-Elastic Neutron Scattering (QENS) experiments and the self-diffusion constant by Nuclear Magnetic Resonance (NMR) experiments. Water is confined in 1-d geometry in cylindrical pores of porous silica materials, MCM-41 and in Double-Wall Carbon Nanotubes (DWNT) [6]. It is in a 2-d geometry as the hydration water on surfaces of biopolymer, protein, DNA, and RNA.

The crossover phenomena can also be observed by measuring the Mean Square Hydrogen Atom Displacement derived from an Incoherent Elastic Neutron Scattering experiment and from appearance of a Boson peak in an Incoherent Inelastic Neutron Scattering experiment. We observe a pronounced violation of the Stokes-Einstein relation at and below the crossover temperature at ambient pressure [2]. Upon applying pressure to the confined water, the crossover temperature is shown to track closely the Widom line emanating from the existence of a liquid-liquid critical point buried in an unattainable deeply supercooled state of bulk water [1]. Relations of the dynamic crossover phenomena to the existence of a density minimum in supercooled confined water [3] and to conformational flexibility of the hydrated biopolymers [4] will be discussed. The crossover temperature is shown to be sensitively dependent on the degree of hydrophilicity of the confining substrate [6]. The crossover phenomenon have also been confirmed by an MD simulation of a hydrated lysozyme powder model [7].

1. Li Liu, Sow-Hsin Chen et al, *Pressure dependence of fragile-to-strong transition and a possible second critical point in supercooled confined water*, PRL **95**, 117802 (2005).

2. Sow-Hsin Chen, Francesco Mallamace et al, *The violation of the Stokes-Einstein relation in supercooled water*, PNAS **103**, 12974 (2006).

3. Dazhi Liu, Sow-Hsin Chen et al, *Observation of the density minimum in deeply supercooled confined water*, PNAS, **104**, 9570 (2007).

4. Sow-Hsin Chen, Li Liu, et. al., *Observation of fragile-to-strong dynamic crossover in protein hydration water*, PNAS **103**, 9012 (2006).

5. Franceso Mallamace and Sow-Hsin Chen et al, *Role of the solvent in the dynamical transitions of proteins:the case of the lysozyme-water system*, JCP **127**, 045104 (2007)

6. Xiang-Qiang Chu, Alexander I. Kolesnikov, A. P. Moravsky, V. Garcia-Sakai, and Sow-Hsin Chen, *Observation of a Dynamic Crossover in Water Confined in Double-wall Carbon Nanotubes,* Physical Review E **76**, 021505 (2007).

7. Marco Lagi and Sow-Hsin Chen et al, *The Low Temperature Dynamic Crossover Phenomenon in Protein Hydration Water: Simulations vs Experiments*, to appear in J. Phys. Chem. B (Letter), 2008.

Some new developments in multidimensional Fourier- and Laplace-inversion NMR

*Paul T. Callaghan, Lauren M. Burcaw, Petrik Galvosas, Daniel Polders
and Kate E. Washburn.*

MacDiarmid Institute for Advanced Materials and Nanotechnology, School of Chemical and
Physical Sciences, Victoria University of Wellington, New Zealand.

In the last five years the use of two-dimensional inverse Laplace Transformation (ILT) methods [1] has become well established in NMR studies of porous media. Indeed, the most powerful applications of multidimensional inverse Laplace spectroscopy may well be in the investigation of fluid displacement in porous media. A particular virtue is the ability to work in low field, as well as high, making these approaches applicable in the widest possible range of NMR from laboratory to portable NMR to bore-hole NMR. Separation, correlation and exchange experiments have been demonstrated, with the Laplace domain traversing T_1, T_2 relaxation, diffusion and internal magnetic gradients, the latter manifest in the decay of echoes due to diffusion in the presence of inhomogeneous local fields. Of course, the ILT does somewhat distort the representation of distributions due to pearling effects, but in a sense, the "binning" of data in this manner can prove quite useful. At the very least, the 2D ILT gives us an excellent means of separation of relaxation and diffusion behavior in complex materials, thus enhancing interpretation and resolution. But it has also given us correlation and exchange analogues of considerable power. All three variants will be traversed here [2-5]. The exchange experiment is particular effective in revealing dynamics through the mixing time dependence of peak intensities [6].

Recently, it has become apparent that the addition of a Fourier dimension can be of particular value. One example is where a 3rd propagator dimension is added. For example, in the case of relaxation exchange a third Fourier dimension relating to molecular displacements can be added [7], allowing spatio-temporal insight regarding spin relaxation for fluid state molecules in porous media [8]. Another example is in the correlation of local fields with relaxation, diffusion and local gradients [9].

An overview of these methods will be presented along with some speculation as to their future potential.

1. Y.Q. Song and L. Venkataramanan, *J. Magn Reson*, (2002) **154** 261
2. P.T. Callaghan and I Fúro, , *J. Chem. Physics*, (2004) **120**, 4032
3. Y. Qiao, P. Galvosas, and P. T. Callaghan*, Biophys. J.*" **89**, 2899-2905 (2005)
4. Y. Qiao, P. Galvosas, T. Adalsteinsson, M. Schönhoff and P. T. Callaghan *J. Chem. Phys* (2005) **122**, 214912-1
5. K.E. Washburn, C.D. Eccles and P. T. Callaghan, *J. Magn. Reson.* (submitted) (2008)
6. K.E. Washburn and P. T. Callaghan, *Physical Review Letters* **97**, 175502 (2006),
7. K.E. Washburn and P. T. Callaghan, *J. Magn. Reson.* **186**, 337-340 (2007)
8. K.E. Washburn, C.H. Arns and P. T. Callaghan, *Phys. Rev. E (in press)* (2008)
9. L. M. Burcaw and P.T Callaghan, *J. Magn. Reson. (submitted)* (2008)

DNP-enhanced NMR analysis of water of soft material assembly

S. Han, E. McCarney, R. Kausik, B. Armstrong

Department of Chemistry and Biochemistry, University of California Santa Barbara, CA

A unique analysis tool for the selective detection of local water inside soft molecular assemblies—hydrophobic cores, amyloid fibers, vesicle bilayers, micelles—contained in bulk water is presented [1]. This was made possible through the use of the Overhauser effect for dynamic nuclear polarization to amplify ^{1}H NMR signal of water through its interaction with stable radical probes that possess ~660 times higher spin polarization compared to ^{1}H nuclei [2-5]. We developed [1]H-Overhauser spectroscopy to provide unique and complementary information to cw electron spin resonance analysis of spin labeled molecular assemblies through the characterization of water interacting with the site-specifically localized spin label [1]. We demonstrate that (1) hydration and water diffusion versus chain dynamics inside bilayer systems can be measured and (2) *tau* protein aggregation to *bona fide* fiber versus non-specific tau agglomeration can be differentiated and dynamically monitored, as only the former involves water exclusion through the formation of hydrophobic regions (Fig.1).
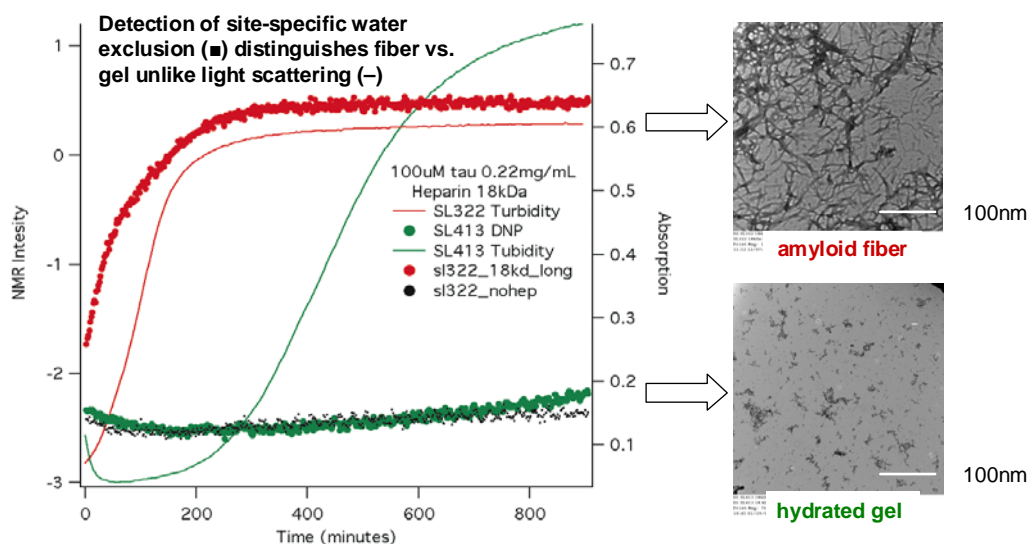

Fig. 1: Tau-187 aggregation monitored by [1]H Overhauser spectroscopy (dotted line), turbidity measurements (straight line) and electron microscopy (pictures) for spin labeled tau-187 mutant SL322 that forms bona fide fibers versus mutant 413 that form non specific agglomerates.

References:

1. E.R. McCarney, B. Armstrong, S. Han, Dynamic nuclear polarization enhanced nuclear magnetic resonance and electron spin resonance studies of hydration and local water dynamics in micelle and vesicle assemblies, Langmuir (2008) in press.
3. K.H. Hausser, D. Stehlik, "Dynamic nuclear polarization in liquids", Advances in Magnetic Resonance 3 (1968), 79-139.
4. I. Nicholson, D.J. Lurie, F.J.L. Robb, "The Application of Proton-Electron Double-Resonance Imaging Techniques to Proton Mobility Studies", J. Magn. Reson. B 104 (1994), 250-255.
5. W. Barros, M. Engelsberg, "Enhanced Overhauser contrast in proton-electron double-resonance imaging of the formation of an alginate hydrogel", J. Magn. Reson. 184 (2007), 101-107.

Microimaging of Catalytic Hydrogenation using Parahydrogen

L.-S. Bouchard,[1] S. R. Burt,[1] M. S. Anwar,[1] K. V. Kovtunov,[2] I. V. Koptyug,[2] T. Theiss,[1] and A. Pines[1]

[1]*Materials Sciences Division, Lawrence Berkeley National Laboratory, Berkeley, CA 94720*
[2]*International Tomography Center, Novosibirsk, Russian Federation.*

We present a MRI method for the study of gas-phase reactions in microfluidic devices. With the use of parahydrogen induced polarization (PHIP) [1] and a novel heterogenized catalyst [2], we are able to provide detailed flow map and visualization of the active regions in an operating catalytic microreactor. This provides a new platform that could be used for the evaluation of novel catalysts and reactors, where their production in very small quantities could result in cost savings [3].

The hydrogenation of propylene gas in a microreactor (continuous flow mode) containing a solid catalyst is visualized (Fig. 1**A**). A mixture of 20% propylene, 40% parahydrogen and 40% orthohydrogen was passed through the catalyst bed. The polarized product, propane, was imaged at 7.1–T. The thermally-polarized protons produced insufficient signal to generate high resolution (sub-mm) images, whereas the PHIP-polarized protons yielded a substantial sensitivity enhancement (Fig. 1**A**). Figure 1**A** is a map of active regions within the catalyst bed. The flow-compensated imaging sequence consisted of a pure phase encoding protocol with zero velocity and acceleration moments. A high resolution flow map (Fig. 1**B**) was produced by velocity encoding along three axes.
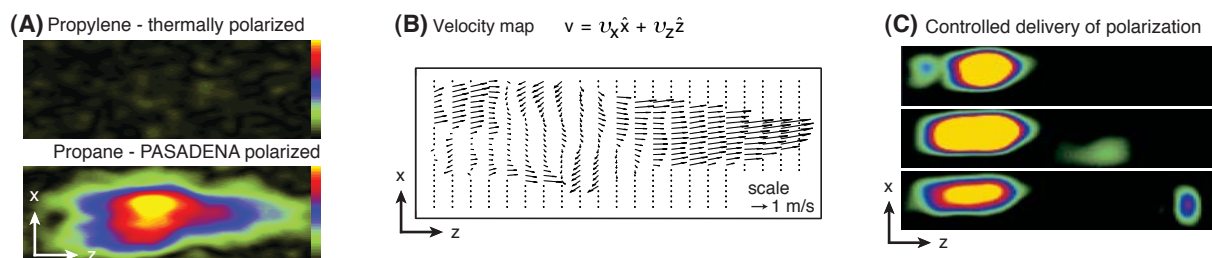

FIG. 1: MRI images of the microreactor during the hydrogenation of propylene into propane by PHIP. (**A**) ^{1}H image of the catalyst bed using thermal propene and polarized propane, (**B**) Flow map (2D projection of the velocity field) of the polarized product, arrows correspond to the direction and magnitude of the velocity at each point, (**C**) Packet of polarized propane released downstream of the catalyst bed, T_d =0, 10 and 40 ms. The field of view is 2.3 by 7mm in Figs. **A** and **B** and 6 by 23mm in Fig. **C**.

Figure 1**C** demonstrates the controlled delivery of polarized product downstream from the catalyst bed with the use of isotropic mixing to prevent the otherwise rapid decay of the singlet states. Mixing allows the polarized product to escape the catalyst bed, which can be imaged after a delay T_d, to allow the product to travel a well-defined distance. These results in gas-phase microflows during a chemical reaction should have applications in chemical engineering, to correlate reactor morphology to active regions within the bed and to probe mass transport within the reactor. The timed release of polarization could also be used to extend the use of PHIP beyond hydrogenation reactions.

---

[1] C. R. Bowers and D. P. Weitekamp, Phys. Rev. Lett. **57**, 2645 (1986).
[2] I. V. Koptyug et al., J. Am. Chem. Soc. **129**, 5580 (2007).
[3] L.-S. Bouchard et al., Science **319**, 442 (2008).

Remotely Detected NMR in Microfluidic Devices with High Spatiotemporal Resolution

Elad Harel, Vik Bajaj, Monica Smith, Alex Pines

Materials Sciences Division, Lawrence Berkeley National Laboratory, and Department of Chemistry, University of California at Berkeley, Berkeley, Californian 94720-1460, USA,

Microfluidics, a technology in which fluid flows are manipulated on short length scales, has delivered integrated "lab on a chip" analytical platforms with increasingly routine applications in molecular biology, synthetic chemistry, and in fundamental studies of fluid dynamics. While analytes are typically detected optically, magnetic resonance (MR) is emerging as a versatile tool in microfluidic applications because spectra rich in chemical information can be acquired without the need for labeling of the analytes. Its principal disadvantages as compared to optical detection are low sensitivity and low time resolution, which limits the time scale of chemical dynamics that can be probed by this technique. The latter is fundamentally set by the time required to observe the NMR spectrum: long observation times are needed to resolve closely spaced resonances, complicating the direct monitoring of fast dynamics. Practically, it is also limited by the geometry of the microfluidic experiment, in which the ratio of
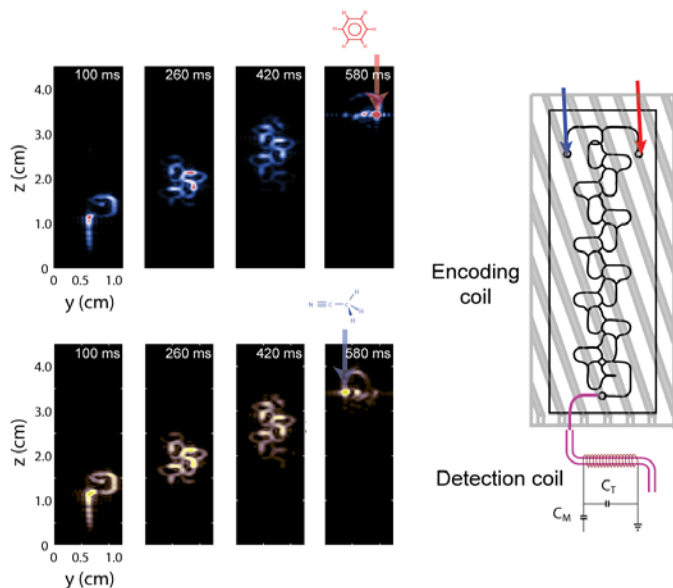

Figure 1. TOF partial images of fluid flow through a lab-on-a-chip device. Information about the spatial origin of each fluid species is encoded and stored along the B_0 axis before stroboscopic acquisition in the detector by a microsolenoid detection coil.

detectable spins to the sensitive volume of the detector is ~10^{-4} or less, precluding the use of fast imaging sequences. Further, magnetic susceptibility gradients imposed by the geometry of the chip and fluid channels dramatically limit the resolution of directly acquired spectra (~10 ppm linewidths) and thus their chemical information content. Here, we demonstrate a variant of remotely detected NMR which overcomes these limitations. By employing spatial encoding of the flowing fluid together with conjugate imaging in the detector coil, we show how high resolution spectra can be acquired with arbitrarily high temporal resolution and several orders of magnitude greater sensitivity than is possible by direct MR measurements. The enhancement is evidenced by recording spectrally resolved fluid mixing through an arbitrarily complex lab-on-a-chip device at 500 frames per second - one of the fasted frame rates recorded in an MRI experiment. This is achieved by combining remote detection NMR with a time 'slicing' of the time-of-flight (TOF) dimension which eliminates the constraints of the limited observation time by converting the time variable into a spatial variable through the use of magnetic field gradients. This method has implications for observing fast processes, such as fluid mixing, with sub millisecond time resolution at micron spatial resolution and as a new modality for on-chip chromatography.

Paramagnetic and Super-paramagnetic Nanoparticles: Magnetic Beacons and Magnetic Bullets for Lesion Detection and Therapy

Yung-Ya Lin
Department of Chemistry and Biochemistry, UCLA, CA, 90095, USA

The strong fluctuating magnetic fields from paramagnetic or super-paramagnetic materials enhance the longitudinal (1/T1) and transverse (1/T2) relaxation rates of surrounding water protons. For examples, in porous media, the additional relaxation dynamics of protons with paramagnetic impurities located on the grain surface provides information about transport processes and characteristic length scales of the pore space. Nanoscale paramagnetic or super-paramagnetic iron oxide (SPIO) cores of magnetite and/or maghemite with appropriate surface chemistry have recently demonstrated their utility in molecular imaging for enhancing MR contrast, allowing researchers to monitor not only anatomical changes, but physiological and molecular changes as well. Applications have ranged from detecting inflammatory diseases via the accumulation of non-targeted SPIO in infiltrating macrophages to the specific identification of cell surface markers expressed on tumors.

In this presentation, our recent methodological developments in applying SPIO as "magnet beacons" for lesion detection and as "magnet bullets" for lesion therapy will be highlighted.

SPIO as "magnet beacons"

(1) Sensitive detection of SPIO by feedback-enhanced magnetic resonance.
Through the use of feedback magnetic fields, active feedback electronic devices, and SPIO's strong microscopic susceptibility effect, we are able to improve the detection sensitivity of early tumor by ~5 times. This is demonstrated by using biomarkers consisting of 50nm SPIO conjugated to mouse anti-carcinoembryonic antigen (CEA) which were injected intravenously through the tail vein of an immune-gene knockout mouse with a human lung cancer (cell line Colo 205) grown in the thigh.

(2) Detection of H5N2 virus by SPIO aggregation.

SPIO as "magnet bullets"

(3) Heating of SPIO in high-frequency magnetic field for electromagnetic hyperthermia.
Hyperthermia is a promising approach to cancer therapy. It is a minimal invasive method for regional selective heat treatment, which is based on heating the target tissue to temperatures between 42 to 46ºC. By this technique, the viability of cancer cells is reduced because they are more sensitive to temperatures above 41ºC than are the normal cells. The magnetic materials generate heat in an alternating magnetic field, which enables the induction of hyperthermia. The sub-domain SPIO particles produce substantially more heat per unit mass than the much larger multi-domain particles of similar composition. The mechanism of heating is based on the Brown effect (rotation of the particle as a whole according to external magnetic field) and the Neél effect (reorientation of the magnetic moment across an effective anisotropy barrier within each particle).

Dispersion in packed beds

U.M. Scheven[a], R. Harris[b] and M.L. Johns[b],

[a]REQUIMTE/CQFB, Departamento de Química, Faculdade de Ciências e Tecnologia, Universidade Nova de Lisboa, Portugal, [b]Magnetic Resonance Research Laboratory, Department of Chemical Engineering, University of Cambridge, UK

The experimental characterization of voidspaces and flow within natural rocks, packed bed reactors, chromatography columns, or in simple packs of mono-disperse solid spheres generally includes measurements of volume averaged properties such as permeability, porosity, dispersivity, and sometimes the hydrodynamic radius $r_h = V/S$, where V and S are the volume and surface area of the pore space respectively. Displacement encoding NMR experiments have made significant contributions to this area of research, with measurements of short time restricted diffusion coefficients yielding the hydrodynamic radius of a pore space[1], and with APGSTE flow propagator[2] and dispersion[3] experiments in packed beds determining pore space dispersivities or effective diffusion coefficients. It is clear, however, that NMR derived dispersivities in packed beds - the one random porous system for which there exist canonical but incompatible theoretical predictions with few or no adjustable parameters[4,5] - can be affected by the same experimental complications which have substantially contributed to the puzzling scatter in published dispersion results based on elution experiments[6]. Notable among these are fast flow near walls, and inhomogeneous flow injection. We will discuss how, with data analysis accounting for these macroscopic flow heterogeneities, an APGSTE-NMR dispersion measurement on flow through a tube of Diameter D packed with monodisperse spheres of diameter d can yield the dispersivities of the infinite pack of spheres, provided d<<D.

References:

1. P.P. Mitra, P.N. Sen and L.M. Schwartz, Phys. Rev. B 47 (1993) 8565.
2. J. Kärger and W. Heink, J. Magn. Res. 51 (1983) 1.
3. A. Ding and D. Candela, Phys. Rev. E 54 (1996) 656.
4. P.G. Saffman, J. Fluid Mech. 7 (1960) 194.
5. D. Koch and J. F. Brady, J. Fluid Mech. 154 (1985) 399.
6. N.W. Han, J. Bhakta and R.G. Carbonell, AIChE J. 31 (1985) 277.

Using Magnetic Resonance to Measure the Interplay of Structure and Transport in Porous Media

Joseph D. Seymour[a,c], Sarah L. Codd[b,c],

[a]Department of Chemical and Biological Engineering, [b]Department of Mechanical and Industrial Engineering, and [c]Center for Biofilm Engineering, Montana State University, Bozeman, Montana U.S.A.

Determination of the structure and transport behavior of porous media is important in fields as diverse as geophysics and biomedicine. Whether modeling the fate and transport of contaminants and oil in the earth's subsurface, or designing ceramics and porous filtration systems for biomedical, energy and environmental applications, an increased understanding of the correlation between porous media structure and transport would allow control of transport by structural modification. Biofouling of porous media due to attached microbial biofilm communities is an important feature of failure in biomedical filtration devices and in controlling subsurface transport with permeability altering biobarriers. Pulsed field gradient magnetic resonance (MR) measurements of the propagator of the motion and corresponding q-space diffraction in bead packs of varying particle to column diameter ratio indicate the impact of ordered packing on transport. Scaling of the effective longitudinal dispersion with Pe^2, the Taylor dispersion dominated regime, is observed in the most ordered bead pack in agreement with theory [1]. Power law scaling of the dispersion coefficient with Peclet number Pe^α decreases with increasing bead pack disorder. Porous media biofouling generates
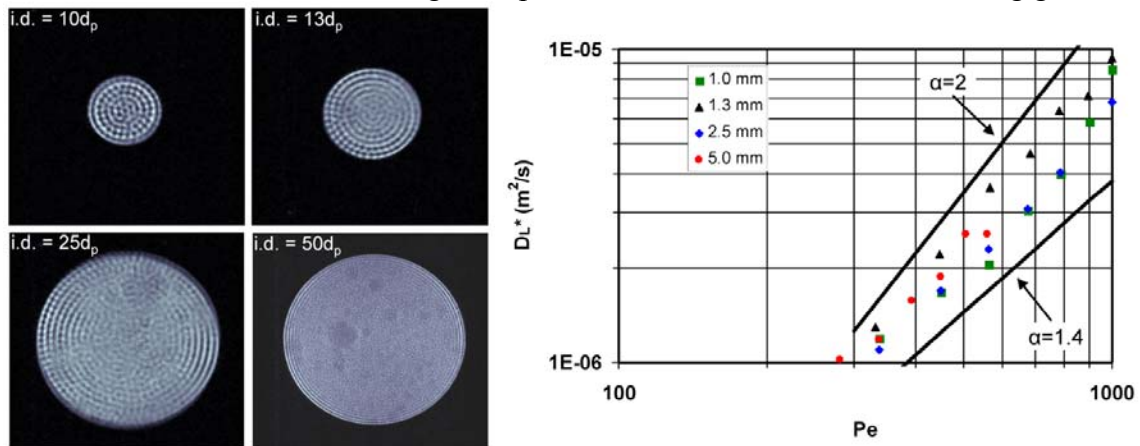

Fig. 1: MR images taken with spatial resolution of 27.3 μm/pixel over an 8 mm thick slice for d_p=100 μm particles in varying diameter columns. The impact of structural ordering on dispersion dynamics as a function of Peclet number is measured. The lines indicate the Taylor Dispersion Pe^2 and power law fit to data Pe^α regimes

a transition in porous media from normal Gaussian transport associated with homogeneous structure to anomalous transport dynamics typical of heterogeneous media [2]. The potential to design porous media with structures in which transport dynamics respond in a controlled fashion to biofouling is considered.

References:

1. D.L. Koch *et al*., The effect of order on dispersion in porous media, J. Fluid Mech. 200 (1989) 173.
2. J.D. Seymour *et al.*, Anomalous fluid transport in porous media induced by biofilm growth, Phys. Rev. Lett. 93 (2004) 198103.

NMR Quantification of Trabecular and Cortical Bone Microstructure and Function

Felix W. Wehrli
Laboratory for Structural NMR Imaging
University of Pennsylvania School of Medicine

Bone is a complex composite material whose strength is determined by a combination of the material's intrinsic mechanical properties, its overall volume fraction and architecture at the macro-, micro- and ultrastructural level. Structure at all scales is governed by the nature of the remodeling process and any imbalance in homeostasis adversely affects the bone's mechanical competence. Trabecular bone, dominant in the vertebrae and ends of long bones, consist of a network of interconnected plates and struts of about 100 µm thickness immersed in a matrix of marrow. The encasing shell of cortical or compact bone is characterized by a system of interconnected channels and pores ranging in width from 100 nm to about 50 µm.

NMR is uniquely suited to probe both trabecular and cortical bone either by direct observation using high-resolution k-space sampling or indirectly by relaxometric techniques and measurement of apparent diffusion. Bone is more diamagnetic than the surrounding marrow (by about 2.5-3ppm S.I.) and the resulting induced magnetic fields in the marrow spaces cause a structure-dependent modulation of the FID from which trabecular density and structural anisotropy can be derived without the requirement for resolving the structures. Direct detection requires resolution sufficient to at least partially resolve individual trabeculae, complicated further by physiologic motion and image noise. It is shown that in combination with image processing it is possible to resolve the 3D architecture of trabecular bone *in vivo* and characterize the bone in terms of parameters of scale and topology, and further, that the method is able to quantify structural changes in response to drug intervention in subjects with osteoporosis. Alternatively, the image data can be fed into a finite element model from which the anisotropic stiffness tensor can be retrieved.

The cortical bone's pore structure is of a scale too small to resolve by NMR. A complicating circumstance is that the protons of water occupying the pores, have extremely short lifetime (<<1ms) caused by both, induced inhomogeneous fields and surface relaxation. We show that by means of solid-state imaging techniques the water content and thus pore volume fraction can be measured, providing a parameter relevant to bone strength. Further insight into the properties of pore water and possibly pore architecture are provided by relaxometric approaches and deuterium NMR, the latter making use of quadrupole splittings resulting from molecular order of collagen-associated water. Lastly, diffusion across the haversian and canalicular system, the sole process available for small-molecule transport between osteocytes and the vascular system, is shown to be accessible through study of H_2O - D_2O exchange kinetics.

In summary, NMR imaging has been shown to provide a wealth of information on bone micro- and nano architecture yielding quantitative insight into its mechanical behavior in health and disease.

Neural Tissue as Porous Media

P.J. Basser

Section on Tissue Biophysics and Biomimetics, NICHD, NIH

MR measurements of molecular displacements and porous media models provide useful information not only about transport properties and microstructure of inanimate porous materials, but also about living tissue, particularly neural tissue.

Hansen's early *ex vivo* measurements of ADCs in nerves were followed by *in vivo* diffusion MRI studies demonstrating diffusion anisotropy in cat and in human white matter (WM). Diffusion tensor NMR and MRI (DTI), based on a Gaussian displacement *PDF*, characterized anisotropic water diffusion in brain WM using maps of material parameters derived from the apparent (or effective) diffusion tensor (ADT). Tuch used cross-property relations to derive an electrical conductivity tensor from this ADT.

Model independent approaches are also useful in characterizing neural tissue structure and organization. Callaghan and Xia's "k- and q-space imaging" method was adapted to clinical scanners by Wedeen (DSI) to estimate a 3-D average propagator in each voxel, providing information about restriction, distinct compartments, etc. The burden of sampling $E(q)$ uniformly throughout 3-D q-space led Tuch to consider functions of the average propagator, e.g., its orientation distribution function (ODF), obtained by collecting $E(q)$ data only over a spherical shell in q-space. Alternatively, Pikalov et al. estimated the 3-D average propagator with less $E(q)$ data by using CT reconstruction methods and *a priori* information.

Several model-based displacement MR approaches have also been used to estimate distinct features of neural tissue. One method treats the extra-axonal space in WM as hindered, described by a DTI model, and the intra-axonal space as restricted. This composite hindered and restricted model of diffusion (CHARMED) MRI framework has been extended to measure the diameter distribution in a pack of axons (AxCaliber), extending and adapting the approach Packer et al. used to estimate the diameter distribution in droplets.

Various porous media approaches have been developed to study gray matter (GM) microstructure. Treating GM as hierarchically organized, exhibiting fractal diffusion, Özarslan et al. proposed scaling relationships for time-dependent displacement distributions; this approach provides a means to estimate several parameters characterizing anomalous diffusion. Viewing dendrites in GM as a network of restricted tubes, Komlosh et al. have applied multiple PFG-MR sequences to measure and characterize *microscopic* diffusion anisotropy in GM, which appears using DTI to be macroscopically isotropic.

Useful analytical and simulation environments have been developed to aid in understanding water transport in neural tissue and its effect on the MR signal. Szafer and Stanisz used Monte Carlo methods in idealized WM to model MR signal attenuation. Wehrli's group used digitized histological WM cross-sections to build more realistic micromodels to simulate diffusive transport and the MR signal attenuation. Frank has developed a computational environment to simulate diffusion in complex media that can treat microstructural heterogeneity over a large range of length scales. Sen et al. developed a model of diffusion within a pack of cylindrical tubes to assess how different microstructural parameters affect the ADCs parallel and perpendicular to the WM fiber axis.

In summary, the use of porous media concepts in conjunction with MR displacement measurements has resulted in the development of novel models and experimental methods to characterize biologically relevant transport properties in neural tissue, and measure microstructural features that otherwise could only be obtained by invasive and tedious histological analysis.

Diffusion MRI of complex order in tissue

Van Wedeen
The Athinoula A. Martinos Center for Functional and Structural Biomedical Imaging,
Massachusetts General Hospital, Charlestown, MA, USA

In the physics of continuous media including condensed physics, it is natural to begin the description with consideration of order parameters; point-symmetry groups in crystals, continuous groups in soft condensed matter, higher dimensional and outright unknown stuff in the vacuum. Living tissues, as examples of ordered matter, present unique examples of complex order. This talk will consider three cases - skeletal muscle, heart and brain - and discuss our attempts to capture their order and disorder with diffusion MRI.

Local anisotropy of tissue is conveniently mapped by q-space diffusion MRI, in which images are acquired of the mean time-dependent propagator of water diffusion at each spatial location x in an NMR image $p(x,r)$ where r denotes spatial displacement and q its Fourier-conjugate. Methods have been proposed in which one either computes a digital image of the entire 3D propagator at each location, effectively a 6-dimensional data set - 3 spatial and 3 diffusion - or which approximate the propagator to second order, by a symmetric diffusion tensor D. Historically, diffusion tensor methods preceded the more general q-space imaging methods by nearly a decade: 1992 vs 2000, resp., causing much difficulty. Following Cory and Garroway, this propagator approximates the spatial autocorrelation of the tissue at each MRI voxel. Beginning with the simplest case, skeletal muscle locally specified by a direction vector at each point. Since these fibers are inversion-symmetric, the set of directions comprise $\mathbb{S}^2/\pm I = \mathbb{RP}^2$. Globally, most skeletal muscles are trivial as fiber bundles - smooth arrays of similar parallel 1D fibers over a 2D base - but there are interesting exceptions. Crossings of fiber populations occur in core of the tongue, where they enable the tongue to elongate as a "muscular hydrostat, and in the wall of the esophagus, where fibers interweave in crossed helices to enable dynamic narrowing of the lumen, in structure and function like Chinese finger cuffs.

Unlike skeletal muscle, the fibers of the myocardium are not discrete elements but a single branching syncytium: the largest single cell. Just like a river that begins in and ends in un-numbered streams and estuaries, myofibers have no defined beginnings or ends, but fan out in a bi-cone of branching though which they couple to their myocardial environment - electrically, chemically and mechanically. This cone is not circular but highly flattened. This flattening separates the myocardium into ribbons of muscle 5-10 cardiac myocytes thick (50-100μ), in humans many mm wide and of unknown length: "myocardial sheets". Globally, myofiber orientations encircle the ventricle, spiraling in toroidal paths concentric to the ventricular mid-wall, a projection to 3D of the canonical action of *exp(it)* in $SU(2) \approx \mathbb{Q}*$ the unimodular quarternions. This special arrangement uniquely allows myocytes throughout the thick ventricular wall to contract equally in ventricular ejection, shortening 11-13%, while generating far larger spatially varying radial strains - thickening - of the wall of the heart that increase smoothly from 20% to 50% from outer to inner wall. Combining MRI of fiber orientation with velocity-sensitive MRI of myocardial 3D strain yields detailed maps of cardiac mechanics for the first time noninvasively, as images, or in humans.

The global structure of the myocardial sheet system is not understood. They comprise non-integrable plane field, for otherwise the heart presumably would disassemble, dilate and fail. However, these planes sit asymmetrically in the ventricle, with alternating left and right pitch over the free and septal walls. The sheets tend to sit at 45° to the radial direction of maximum thickening and form a dense slip-system for cellular rearrangement, to augment myocardial compliance, yet their motion has never been directly observed. It is known that sheet structure may be compromised or lost entirely following cardiac damage, associated with increased myocardial stiffness and reduced function.

While structure of cardiac and skeletal muscle is well represented by a second-order diffusion tensor - fiber orientations by leading eigenvectors of diffusion tensors, sheet orientations by second eigenvectors – such tensors fail to capture the complex fiber architecture of neural tissue, particularly the brain. In particular, at scales accessible to MRI crossing fibers are indispensable to neural tissue. Fortunately such fiber structure can be accurately captured by q-space diffusion MRI. Numerical integration of fiber orientation fields in the brain, "tractography", has produced the first maps of fiber pathways in the human brain. This method is now becoming a clinical standard in pre-surgical planning. The fiber pathways of the brain display striking and beautiful 3D order and symmetry, reflecting developmental history as well as their organizing principles as at once a logical, topological and physical network. While multi-fiber order seems appropriate and possibly sufficient for mapping white matter, the geometric order of gray matter including the cerebral cortex is not yet known. To conclude, diffusion MRI of fiber structure in tissue recasts familiar anatomy as the shadow order that freely extends into more than 3 dimensions.

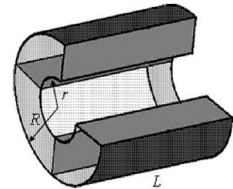# Models and Applications of In Vivo Lung Morphometry with Hyperpolarized ^{3}He MRI in a Mild COPD Population

J. Quirk[a], A. Sukstanskii[a], B. Lutey[b], D. Gierada[a], J. Woods[a,c], M. Conradi[a,c], D. Yablonskiy[a,c]

[a]Mallinckrodt Institute of Radiology, [b]Department of Pulmonology, [c]Department of Physics, Washington University, St. Louis, MO

Hyperpolarized ^{3}He diffusion MRI is increasingly used to non-invasively quantify local alveolar structure changes, such as those from Chronic Obstructive Pulmonary Disease (COPD). Previously [1], we described an in vivo lung morphometry technique that decouples the helium apparent diffusion coefficient (ADC) into components oriented along the longitudinal (D_L) and transverse (D_T) axes of the acinar airways. The measured MRI signal is modeled using Eq. (1), where Φ is the error function.

$$S(b) = S_0 \exp\left[-bD_T \left(\frac{\pi}{4bD_{AN}} \right)^{1/2} \cdot \Phi\left[bD_{AN}^{1/2} \right] \right]; \quad D_{AN} = D_L - D_T \qquad (1)$$

More recently [2], we expanded this theory to express helium diffusion in terms of the airway radii. In Weibel's model of the lung [3], acinar airways are treated as cylindrical objects covered by an alveolar sleeve, defined by its inner (r) and outer (R) radii. In histological measurements of healthy human lungs at 90% of TLC, the mean $r \approx 160$ μm and the mean $R \approx 350$ μm [3]. Following this model, we simulated airways as a periodic structure of cylindrical symmetry (shown right with one of the four alveoli removed). These computer simulations revealed remarkable scaling relationships and allowed us to represent the anisotropic apparent diffusion coefficients (D_L and D_T) in a rather compact form. They also demonstrated the dependence of these ADCs on the *b*-value:

$$D_L = D_{L0} \cdot (1 - \beta_L \cdot bD_{L0}), \quad D_T = D_{T0} \cdot (1 + \beta_T \cdot bD_{T0}) \qquad (2)$$

where D_{L0}, β_L, D_{T0} and β_T are functions of the model parameters, the diffusion-sensitizing gradient waveform, and D_0, the free diffusion coefficient of helium-3 gas in air. To gain insight into the mechanisms of early COPD, we applied this theory to helium diffusion data acquired from thirty "asymptomatic" subjects with significant smoking histories (50 ± 20 pack years, average age 62 ± 3 years) recruited from the National Lung Screening Trial, and five healthy non-smokers (average age 34 ± 4 years). All procedures were performed with IRB approval and ^{3}He MRI was performed under a ^{3}He IND FDA exemption.

In normal subjects, the mean airway inner and outer radii determined from the MRI measurements were 170 ± 30 and 310 ± 40 μm. Given that our measurements are performed at about 60% of TLC, they are in a very good agreement with histology measurements [3]. The helium diffusion measurement showed increased mean internal radii in twenty five smokers (mean 240 ± 40 μm) and increased mean external radii in six (mean 325 ± 30 μm). Significant heterogeneity in these parameters was seen across the lungs in the majority of smokers. Regions of increased internal radii were typically more extensive than regions of increased external radii, suggesting that the inter-alveolar walls were damaged in this population prior to gross airway dilation.

References:

[1] D. A. Yablonskiy, Proc Natl Acad Sci U S A (2002), 99, 3111-6
[2] A. L. Sukstanskii and D. A. Yablonskiy, J Magn Reson (2008), 190, 200-10
[3] B. Haefeli-Bleuer and E. R. Weibel, Anat Rec (1988), 220, 401-14

Nuclear Magnetic Resonance Applications to Unconventional Fossil Fuel Resources

R.L. Kleinberg and G. Leu
Schlumberger-Doll Research, Cambridge, Massachusetts

Technical and economic projections strongly suggest that fossil fuels will continue to play a dominant role in the global energy market through at least the mid twenty-first century. However, low-cost "conventional" oil and gas will be depleted in that time frame. Therefore new sources of energy will need to be developed. We discuss three relatively untapped unconventional fossil fuels: heavy oil, oil shale, and gas hydrate. In each case, nuclear magnetic resonance technology can play a key role in appraising the resource and/or providing information needed for selecting production processes.

Heavy oil is a degraded form of petroleum found in extensive earth formations relatively near the surface. One of the principal physical properties controlling its exploitation is its viscosity. Viscosities of exploitable oils range from less than 1 mPa-s to more than 1,000,000 mPa-s (1 mPa-s = 1 centipoise). As long ago as 1948, Bloembergen, Purcell, and Pound showed that NMR relaxation times are sensitive to the viscosity of fluids. In recent years it has become possible to measure NMR relaxation times in earth formations *in situ*. However, heavy oils are complex fluids with magnetization decays that are grossly nonexponential. Moreover, as found in the earth, they are frequently mixed with water, which also relaxes nonexponentially due to interactions with minerals that form the rock matrix. We have developed laboratory and borehole methods that allow us to use NMR measurements to estimate the viscosity of oil, even when the oil is mixed with water in the pores of natural rock.

Oil shale is a mixture of fine sediments and kerogen, which is organic matter that has not been subjected to temperatures and pressures sufficient to convert it to petroleum. An immense quantity of oil shale accumulated in a lake covering several counties in Colorado, Utah, and Wyoming in the Eocene epoch, approximately 55 million years before present. Kerogen must be heated to high temperature in order to convert it to oil and gas at economic rates. An NMR assay of water content is potentially an important input into production process selection.

Gas hydrate is an ice clathrate that traps methane and other natural gases at elevated pressures and temperatures above 0°C. Substantial quantities have been found in and below permafrost, and under the seafloor at all latitudes. Building on novel experiments performed on a submarine, and on a drilling rig on the North Slope of Alaska, NMR has been used to determine how much gas hydrate is present in arctic and deep water accumulations.

Portable Quadrupole Resonance Systems

Hector Robert
Product Development Manager - Quantum Magnetics, Inc.
15175 Innovation Dr, San Diego, CA 92128 USA

Quadrupole Resonance (QR) sensors have the unique capability of detecting explosives with remarkably high detection rates and low numbers of false alarm. This presentation describes some of the technical and scientific accomplishments at Quantum Magnetics, Inc., a wholly-owned subsidiary of GE Homeland Protection, that resulted in the fabrication of handheld, portable QR systems for effective detection of energetic materials under field conditions. A number of difficulties that impact operation in the field—such as external radio-frequency interference (RFI), inhomogeneity of the excitation fields, and line broadening due to temperature effects—have been mitigated to achieve the highest possible detection performance with the lowest number of nuisance alarms. This presentation describes some of these developments and presents results that demonstrate their usefulness for improved QR system operation in the field.

CMOS mini-NMR biomolecular sensor

Donhee Ham
Division of Engineering & Applied Science
Harvard University, Cambridge, MA

My research group, in collaboration with Ralph Weissleder's group at Massachusetts General Hospital, has recently developed the smallest complete NMR relaxometry system ever built, at the heart of which lies a sophisticated silicon RF chip that can elaborately manipulate water proton spins and monitor their relaxation dynamics. It can detect biomolecules (e.g., cancer marker proteins) in a sample (e.g. blood), by monitoring water (most bio samples contain a large number of water molecules) proton spin dynamics affected by the biomolecules. This work is marked with drastic size reduction and sensitivity enhancement. A state-of-the-art benchtop NMR relaxometer is heavy (120 kg) and bulky (100-liter), due to a large magnet and discrete RF electronics used. Our system weights only 2 kg (60 times lighter) and occupies 2.5 liter (40 times smaller), while achieving 60 times better mass sensitivity. This was made possible by using a small, fist-size magnet, but more crucially, by integrating RF electronics onto the silicon CMOS chip. The design challenge we overcame was attaining RF performance far beyond what would be typically sufficient for larger NMR systems, in order to detect and analyze NMR signals severely degraded by the small magnet. This system can be used as a general NMR relaxometry system, or for diagnostic analysis, in the small, portable platform at low cost, brought closer to patients and doctors.